TRACTOR TRAILER AERODYNAMICS

By

VIKRAM MANTHRI

A THESIS PRESENTED TO THE GRADUATE SCHOOL
OF THE UNIVERSITY OF FLORIDA IN PARTIAL FULFILLMENT
OF THE REQUIREMENTS FOR THE DEGREE OF
MASTER OF SCIENCE

UNIVERSITY OF FLORIDA

2013

Dedicated to my family for their love and support.

ACKNOWLEDGMENTS

I would like to thank Dr. H.A. Ingley and Dr. Subrata Roy for giving me the opportunity to work with them and to participate in the research. Their constant guidance, support and motivation was invaluable. In addition, I would like to thank all the members of the Applied Physics Research group and my friend Karthik for their academic help and suggestion.Most important of all, I would like to express my gratefulness to my parents, sister and brother for their constant support and blessings.

TABLE OF CONTENTS

LIST OF TABLES

Table page

LIST OF FIGURES

Figure page

LIST OF ABBREVIATIONS

BSL	Baseline
CFD	Computational Fluid Dynamics
DES	Detached Eddy Simulation
DOT	Department of Transportation
FMG	Full Multigrid initialization
FHWA	Federal Highway Administration
GTS	Ground Transportation System
HOTR	Higher Order Term Relaxation
LES	Large Eddy Simulation
PIV	Particle Image Velocimetry
RANS	Reynolds-averaged Navier-Stokes
RF	Relaxation Factor
SA	Spalart-Allmaras
SST	Shear Stress Transport

LIST OF SYMBOLS

Cp	Coefficient of Pressure
Cd	Drag Coefficient
k	Turbulent kinetic energy
m	metre
Pa	Pascal
Re	Reynolds number
sec	seconds
u	X component of velocity
v	Y component of velocity
w	Trailer width (32.38 cm)
x	X coordinate
y	Y coordinate

Abstract of Thesis Presented to the Graduate School
of the University of Florida in Partial Fulfillment of the
Requirements for the Degree of Master of Science

TRACTOR TRAILER AERODYNAMICS

By

Vikram Manthri
December 2013

Chair: H.A. Ingley
Major: Mechanical Engineering

Heavy trucks' petroleum consumption is around 12% of the total US petroleum usage. At highway speeds, 65% of this energy is consumed by the trucks in overcoming the aerodynamic drag. So, reducing the aerodynamic drag will not only save money but will also make US less dependent on foreign oil. Present available devices like boattails, side skirts, side and roof extenders, gap fillers, splitter plates etc do not reduce the drag significantly. In addition, many of these devices have operation and maintenance problems. So, there is a need for the development of new devices.

In order to see the effect of boundary layer manipulating devices at the blunt base of the trailer, accurate prediction of the wake is necessary as the pressure drag is the major contributor of the aerodynamic drag. In this thesis, a turbulence model study has been performed on GTS to predict the wake structure. It was found that RANS models are not good enough for predicting the wake structure. Furthermore, DES model was also not able to predict the wake similar to NASA experiment but as the simulation was carried out on a coarse mesh, it should be further studied in order to reach to a conclusion.

CHAPTER 1
INTRODUCTION: PROBLEM DESCRIPTION

The world today is facing serious energy crisis. The dwindling oil and gas resources along with the current state of less reliable renewable energy sources and the increasing gas prices pose a serious challenge on the world countries.

According to US DOT [1] and FHWA[2] , US consumes 18.84 million barrels of petroleum per day which is 21.6 % of the World's petroleum consumption. At the same time, US produces only 9.5% of the World's petroleum. So, US has to depend on foreign countries for oil. In order to decrease the oil dependency, Energy reduction and conservation methods are the need of the hour. Transportation sector accounts for 67% of total US petroleum usage. There are around 10.77 million heavy trucks registered and they travel ~140 billion miles on interstate highways and freeways in a year. These Heavy Trucks consume about 18% of the transportation petroleum which is ~12% of the total US petroleum usage. The division of US petroleum use for the transportation sector can be seen Figure 1-1.

Most of the energy consumed by these trucks is used to overcome the aerodynamic drag and the rolling friction. But the power consumed to overcome the aerodynamic drag increases rapidly with increase in the speed of the vehicle as compared to the rolling friction. For a typical highway speed, aerodynamic drag accounts for 65% of the total power consumption[3].

According to Wikipedia[4], the aerodynamic drag can be categorized into form drag and skin friction. The form drag is due to the size and shape of the object. Bodies with larger frontal area tend to experience more form drag than ones with less. Skin friction is due to the friction between the fluid and the surface of the body. Figure 1-2

shows the variation of form drag and skin friction for bodies with different frontal area. It can be seen that as frontal area increases, the body will experience more form drag than skin friction. For vertical flat plate, the form drag is almost 100 % while the skin friction is negligible.

The problem with tractor trailer is similar in nature. They have large frontal area, both the tractor as well as the trailer. As a result, the drag experienced by the tractor trailer is mostly due to the form drag. Streamlining the body to reduce the frontal area is one of the solutions to reduce the form drag. This had been employed by the car manufacturers for many years now. Cars have been streamlined for years for reducing the form drag [5] [6]. Similarly the tractor had been streamlined to reduce the form drag in front of the vehicle [7] but there is a problem with the trailers, the cargo space. For any given dimensions, the box shape has the highest volume. As a result, for being able to carry as much as cargo as possible, the containers behind the truck cannot be streamlined.

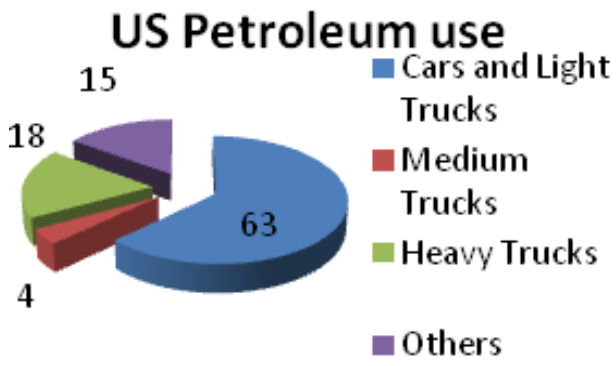

Figure 1-1. US petroleum consumption

Shape and flow	Form drag	Skin friction
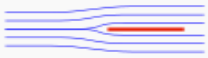	0%	100%
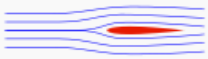	~10%	~90%
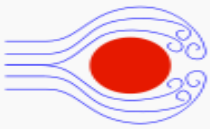	~90%	~10%
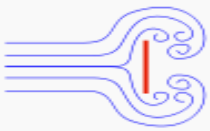	100%	0%

Figure 1-2. Effect of shape on skin friction and form drag (Wikipedia)

CHAPTER 2
PRESSURE DRAG ON A TRACTOR TRAILER

There are 4 areas on a tractor trailer which experience pressure drag, the front portion of the tractor, undercarriage of the trailer, gap between tractor and trailer and the rear end of the trailer. The areas can be seen in the Figure 2-1.

As the truck moves through the air, there is a large pressure drop on front of the tractor as the air imparts momentum to it in opposite direction of travel. The amount of pressure loss can be decreased by the streamlining the tractor.

The gap between the tractor and trailer is another major concern particularly in the cross flow. The air gets entrapped in the gap creating low pressure vortices and imparting the momentum to the truck in its opposite direction of travel. Various devices have been developed to reduce the entrapment as well as to increase the pressure. Base bleeding [8] involves blowing the air through the base of the tractor. The blowing of air alters the vortex structures and thus changing the pressure in the tractor trailer gap. Cabin side extenders which are typically vertical plates installed on the tractor base reduce the gap drag by blocking some of the flow entering into the tractor trailer gap. Rooftop aero-shield deflectors, trailer mounted vortex stabilizer, gap fillers and sealers are some of the other devices for reducing the gap drag [9] [10].Most of these devices except the base bleeding technique have maintenance and operational issues due to which they have not been installed on the modern vehicles.

The undercarriage of a tractor trailer hosts a huge number of devices viz. axles, wheels etc which acts as bluff bodies causing the pressure drop. Also, there is a cross flow as well as the axial flow of air. The complex geometries and the flow nature make the flow really complex and unsteady in nature. Different types of skirts viz. side skirts,

long wedge skirt, short wedge skirt etc [11] have been developed to prevent the crossflow of air entering into the undercarriage and thus reducing the drag. Various front fairings and rear fairings [12][13] for rear axle have been developed to block the flow from the axle and reduce the drag.

As the air moves along the trailer, it separates from the blunt base of the trailer and forms 2 vortex structures. The low pressure created by this separation and the formation of the wake causes the drag on the tractor trailer. Some of the methods for reducing this base drag are boat tailing, base bleeding and boundary layer manipulating devices.

Boat tailing involves gradual reduction of the cross section at the rear end of the bluff body (trailer in this case). This changes the way the streamlines are bent after separating from the blunt base and when they approach the axis of wake, causing the pressure increase. Boat tailing also decreases the size of the wake. Many devices have been developed and tested based on this concept. Inflatable boat tail [14]and base flaps [15] [16] [17] are the some of the devices which come under this category.

Boundary layer manipulating devices are used for delaying or preventing the separation of boundary layer from the wall. We know that the flow separation occurs when we have a flow against an adverse pressure gradient and the fluid loses its momentum in the boundary layer compared to the wall. These devices tend to impart an extra momentum to the fluid in the boundary layer and thus delaying the flow separation. Vortex generators [18] and plasma actuators are some of the devices which come in this category.

Most of the available devices like boat tails, skirts, side extenders, gap fillers and vortex generators do not reduce the drag significantly. In addition, many of these devices also have operation and maintenance problems. As a result, there is a need for new drag reduction device.

In this study, aerodynamics of a tractor trailer had been discussed and a study of turbulence models had been performed. This study can be used further to test the effectiveness of new devices to manipulate the wake behind the trailer.

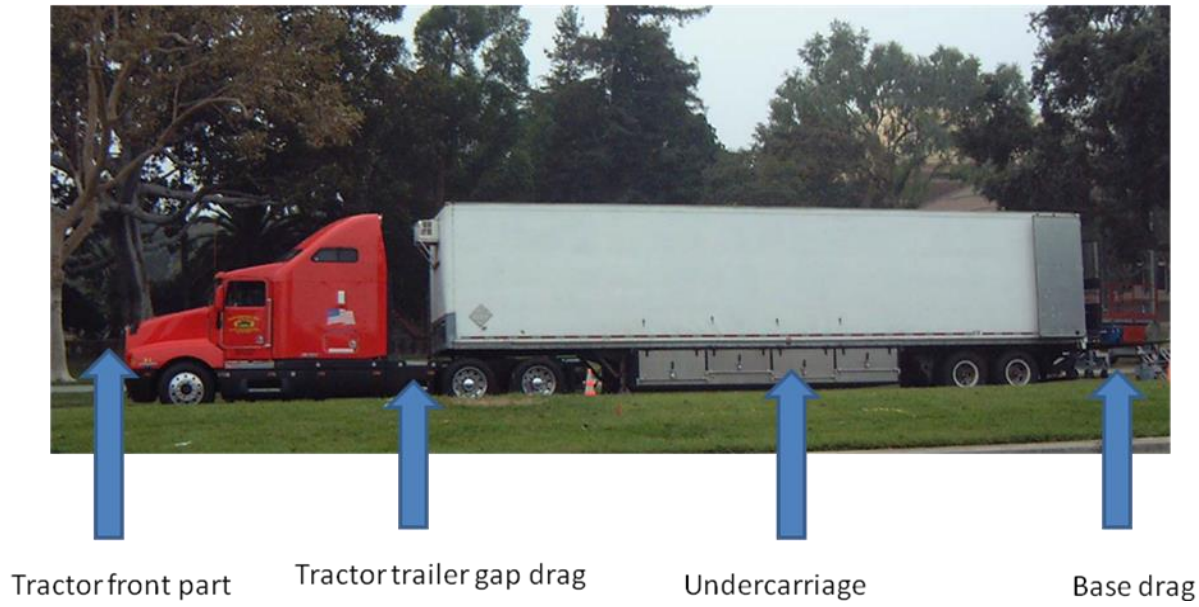

Figure 2-1. Various areas of a tractor trailer contributing to the pressure drag

CHAPTER 3
NASA EXPERIMENT AND FURTHER RESEARCH

NASA Experiment and GTS Model

NASA Ames Research Center conducted a study [19] on 1/8th scale GTS model in their 7 X 10 ft wind tunnel for obtaining experimental data which can be used for the purpose of CFD validation.

GTS is an aerodynamically simplified model of a tractor trailer. It is a cab over engine design with no tractor trailer gap. It is a 1/8th scale model of a class 8 tractor trailer with no wheels and is resting on the four cylindrical posts.

The experiment included measuring body-axis drag, surface pressures, surface hot-film anemometry, oil-film interferometry, and 3-D PIV. They studied the effect of boat tails on the tractor trailer drag. The wind averaged drag coefficients with and without boat tails were found to be 0.225 and 0.277.Reynolds number study (0.3-2 million) was also carried out and they found that that the drag coefficient varied significantly below Re 1 million which involved less variation in base pressure coefficient and more in front of the model. These results were used for validating the CFD simulation results.

Further Research

K. Salari et al.[20] found that the converging section of the wind tunnel was enough to capture the incoming boundary layer. So, he excluded the settling chamber of the wind tunnel.

He performed simulations using SA and k-epsilon turbulence model. As NASA experiment did not provide data at the outlet, he found the outlet pressure by iterating it until he matched the values of the experiment at the test section. He found that the

pressure coefficients predicted at the front, rear, bottom of the truck showed good agreement with the experimental results while at the base of the truck, it showed different trend. He also concluded that the size of the wake behind the trailer is sensitive to the turbulence model.

The drag coefficients that he predicted with k-epsilon and SA turbulence model were 0.318 and 0.418 with 21% and 59% error respectively from the experimental value. He mentioned that he faced convergence issues with k-epsilon turbulence model. Also, SA turbulence model predicted the drag coefficient with 44% error for coarse mesh while for medium mesh it was 59 % error. This clearly shows that there is a problem with the SA turbulence model in drag prediction, as generally the drag prediction improves with refinement.

C.J. Roy et al. [21] found that at Re 2 million, RANS Menter BSL k-omega turbulence model (almost identical to Menter k-omega SST model) provided good drag estimate while it predicted poorly at low Re 22000. He also found out that the surface pressure predicted is close to everywhere except in the base region. The simulation predicted a symmetrical pair of counter rotating vortices in the vertical central line plane in the wake while the experimental data showed asymmetric pair. He also suggested that RANS model is not good enough to predict the effect of drag reduction devices which alter the near wake structure. The drag coefficients that he predicted with Menter k-w and SA turbulence model were 0.298 and 0.413

CHAPTER 4
PROCEDURE AND CFD CODE

Procedure

In NASA experiment, the pressure coefficient had been calculated using a reference pressure at a reference point on the side wall of the wind tunnel. The reference point is located at x/w =4.47, y/w=2.59 and z/w=-4.7, where w is the trailer width and the origin is located in front of the GTS at mid plane. The pressure coefficient [21] is defined as

$$Cp = \frac{(p - p_\infty)}{0.5 * rho_\infty * u_\infty^2}$$

Therefore in order to validate the results with the experimental results, NASA Ames 7X10 ft wind tunnel was modeled and the same reference point was used for calculation of pressure coefficient.

Also, static pressure was not measured at the outflow of the tunnel in the NASA experiment. For obtaining this boundary condition, empty wind tunnel simulations were performed first. In these simulations, the outflow static pressure value was iterated until the static pressure and Mach number at the reference point reaches the experimental value. Then the boundary layer profile at the entrance to the test section of the wind tunnel was matched.

After obtaining the outflow conditions, GTS simulations with RANS and DES turbulence models were performed.

CFD Code

For carrying out CFD simulations, Ansys workbench - a commercial CFD package, was used. Modeling was done using Designmodeler, Meshing was done using

Ansys Meshing and simulation was performed using Ansys Fluent, all of which are integrated into Ansys workbench. Ansys Fluent is a finite volume solver. The post processing was done in Tecplot360 and CFD post.

CHAPTER 5
EMPTY TUNNEL SIMULATION

Geometry

The geometry of the NASA 7X10 ft empty wind tunnel was obtained from C.J. Roy and was modeled using Ansys Designmodeler. It was shown by K. Salari that only a part of the wind tunnel was enough for simulating the flow. The wind tunnel has a 15 ft long test section that is 7 ft in height and 10 ft in width.

Half of the wind tunnel was modeled about the symmetry plane. The inlet was taken as pressure inlet and outlet as pressure outlet. The bottom wall (road) was taken as no slip wall and the top and right walls were modeled as slip walls. The domain has been extended by a unit length at the inlet and outlet due to convergence issues. The modeled wind tunnel can be seen in Figure 5-1.

Meshing

Unstructured grid was used for meshing. The meshing was produced by patch conforming tetrahedron algorithm along with curvature and proximity advanced sizing functions. Inflation layers (boundary layers) were added on the road. The first inflation layer thickness was given as 3e-6 m (estimated from turbulent flow over a flat plate). The mesh for obtaining outlet pressure simulation included 30 inflation layers with 20 % growth rate. Later on, in the boundary layer correction simulation 45 inflation layers with 20% growth rate were included in the mesh. Both meshes can be seen in Figure 5-2, Figure 5-3 and Figure 5-4.

Physics

The flow was assumed to be as compressible and the air as an ideal gas. Density based solver was used and the steady state solution was obtained. For

turbulence, RANS k-omega SST model was selected. The flow was initialized with standard initialization and then FMG initialization was performed with 5 cycles and a RF of 0.75. Pseudo Transient with a time step of 0.001 sec and HOTR with a RF of 0.25 were also activated. For the first 100 iterations, first order upwind scheme was used for discretisation and then second order upwind scheme was activated.

Results

Table 5-1 shows the results for obtaining the outlet pressure and the mesh independent study. Four meshes, coarse mesh with 0.24 million cells, Medium mesh with 0.44 million cells, Refine1 mesh with 1 million cells and Refine2 mesh with 1.7 million cells have been studied. The simulations involved iterating the outlet pressure until the test section conditions of static pressure = 97582 Pa, Mach number =0.27 were obtained for each mesh. The residuals were reduced until 10e-6 and the reference point values were monitored for confirming the steady state solution. The outlet pressure did not vary much (4 Pa) as we refined from coarse mesh to Medium mesh but the outlet pressure did reduce by 350 Pa as we refined the mesh from Medium to Refine1 and then by 200 Pa as we refined the mesh further from Refine 1 to Refine 2. Medium mesh with 0.44 million cells was selected as Mesh independent solution due to limitation in computational resources.

In order to match the boundary layer at section with that of experiment, Medium mesh was then modified with additional inflation layers and then flow was simulated. The outlet pressure was again iterated until the test section values were matched with the experiment. It can be said that that boundary layer profile is independent of the outlet pressure as the outlet pressure did not change much. The results from the boundary layer correction simulation can be seen in Table 5-2.

It can be seen from the x velocity isoplot (Figure 5-5), pressure isoplot (Figure 5-6) and the pressure contour (Figure 5-7) that the velocity and pressure are uniform in the test section of wind tunnel. V velocity contour and W velocity contours (Figure 5-8) clearly show that the velocity in y and z directions is negligible in the test section.

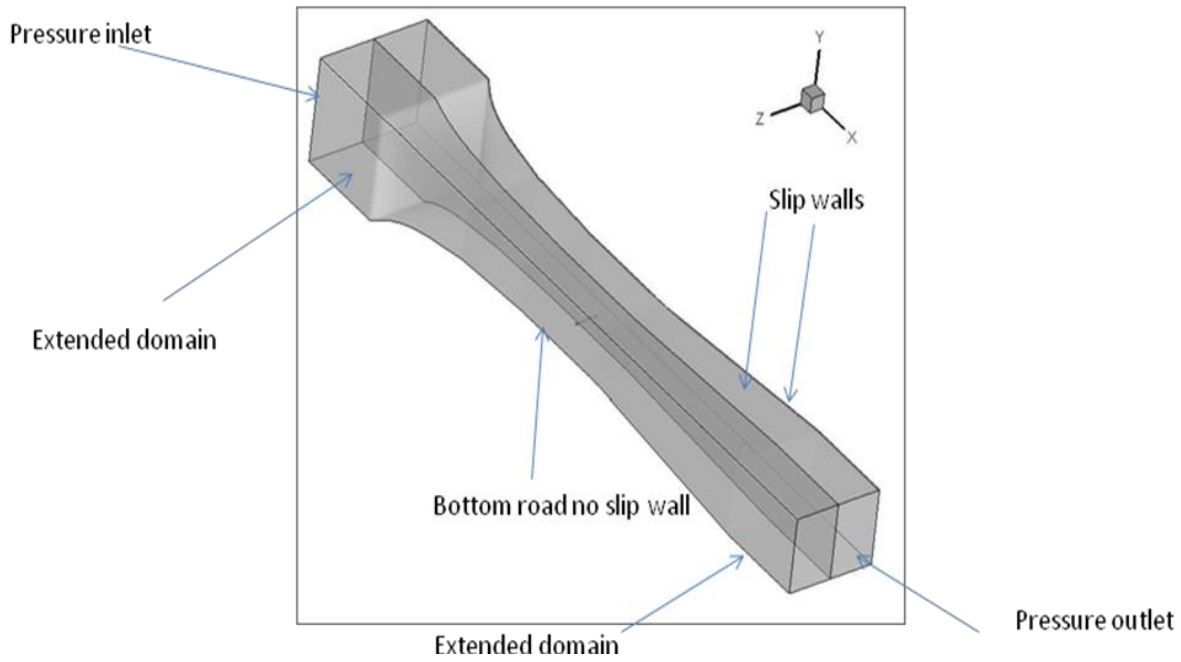

Figure 5-1. Wind tunnel geometry with boundary conditions.

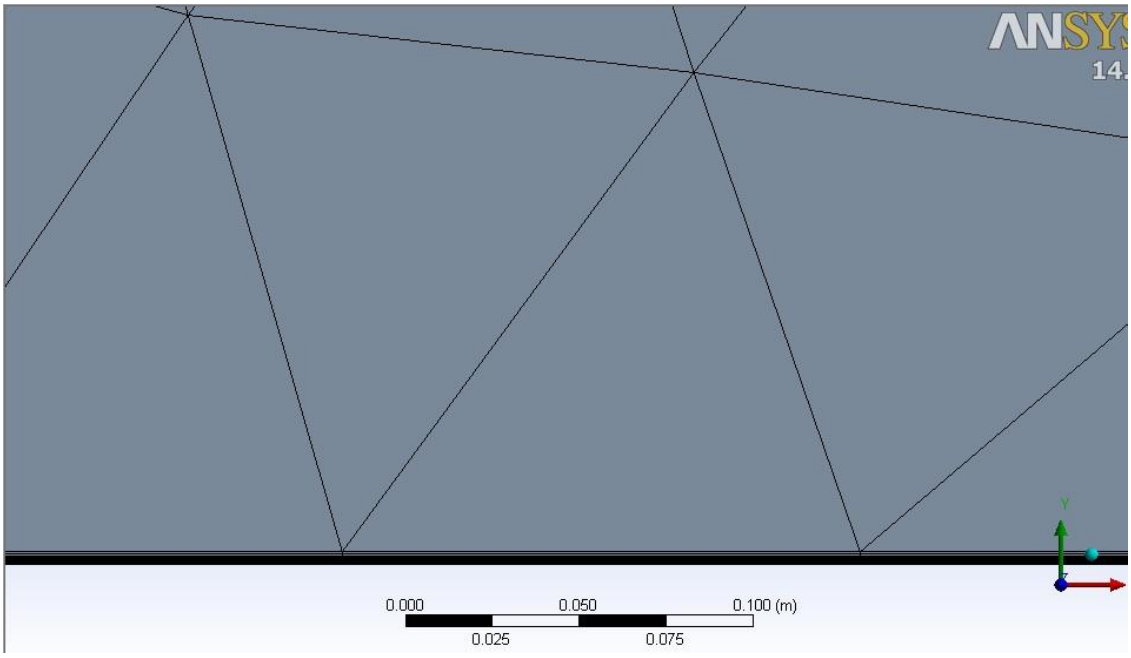

Figure 5-2. Mesh with 30 inflation layers.

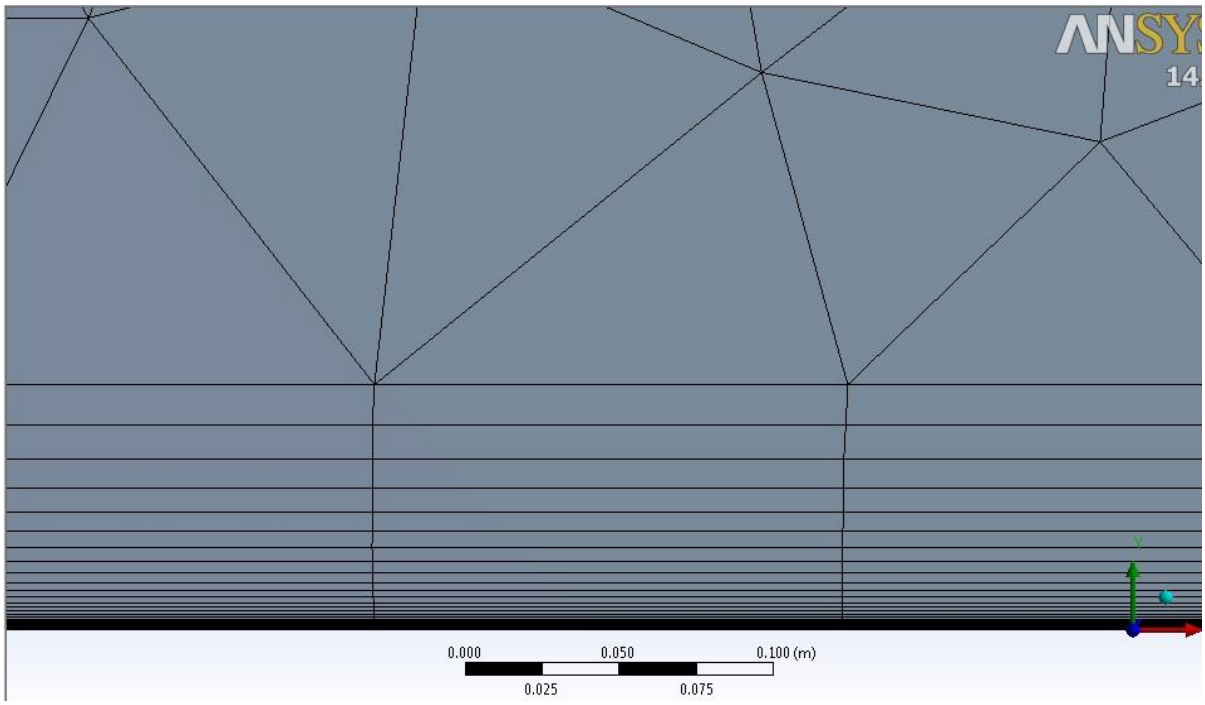

Figure 5-3. Mesh with 45 inflation layers for boundary layer correction simulation.

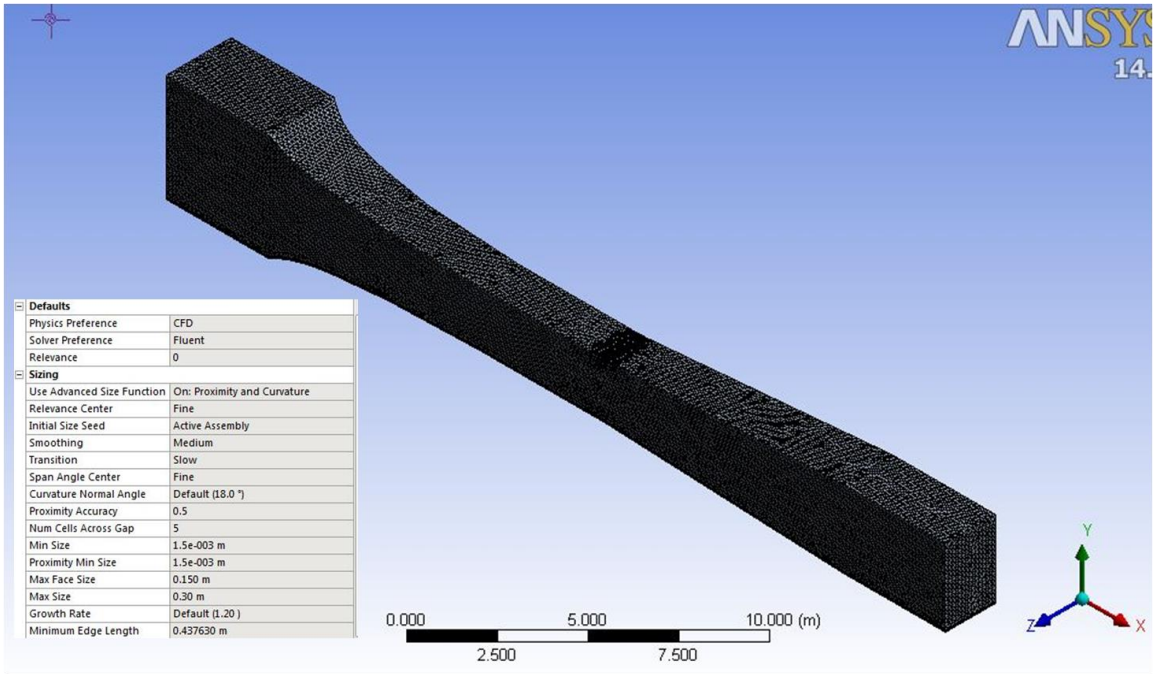

Figure 5-4. Mesh with advance function settings.

Table 5-1. Results of simulations for obtaining outlet pressure conditions.

Mesh	case	Nodes	Elements /cells	inlet stagnation pressure (in Pa)	inlet stagnation temperature (in K)	test static pressure (in Pa)	test velocity (in m/s)	Mach no	Outlet pressure (in Pa)	y+(road)	Pseudo time step (in sec)
coarse	case1	87245	240638	102653.2	282	97555	90.224	0.27006	101002.5	0to3	0.001
coarse	case2	87245	240638	102653.2	282	97580	89.994	0.26936	101010.6	0 to 3	0.001
coarse	case 3	87245	240638	102653.2	282	97582	89.977	0.26931	101011.2	0 to 3	0.001
medium	case1	150781	439975	102653.2	282	97568	90.124	0.26975	101011.2	0to3	0.001
medium	case2	150781	439975	102653.2	282	97583	89.99	0.26935	101015.5	0 to 3	0.001
medium	case 3	150781	439975	102653.2	282	97582	89.997	0.26937	101015.2	0 to 3	0.001
Refine 1	case1	330510	1014008	102653.2	282	98286	83.475	0.2496	101015.2	0 to 3	0.001
Refine 1	case2	330510	1014008	102653.2	282	97717	88.841	0.26586	100802.5	0 to 3	0.001
Refine 1	case 3	330510	1014008	102653.2	282	97582	90.0067	0.26958	100752	0 to 3	0.001
Refine 2	Case1	529967	1696828	102653.2	282	98024	85.97	0.25715	100752	0 to 3	0.001
Refine 2	case2	529967	1696828	102653.2	282	97628	89.635	0.26827	100587	0 to 3	0.001
Refine 2	case 3	529967	1696828	102653.2	282	97582	89.995	0.26935	100567.8	0 to3	0.001

Table 5-2. Results of the boundary layer correction simulation.

Mesh	Case	Nodes	Elements/cells	inlet stagnation pressure (in Pa)	inlet stagnation temperature (in K)	test static pressure (in Pa)	test velocity (in m/s)	Mach no	Outlet pressure (in Pa)	y+(road)	Pseudo time step (in sec)
Medium	case 1	207121	543661	102653.2	282	97557	90.234	0.27009	101015.2	0 to 0.35	0.001
Medium	case 2	207121	543661	102653.2	282	97580	90.024	0.2945	101022.4	0 to 0.35	0.001
Medium	case 3	207121	543661	102653.2	282	97582	90.007	0.2694	101023	0 to 0.35	0.001

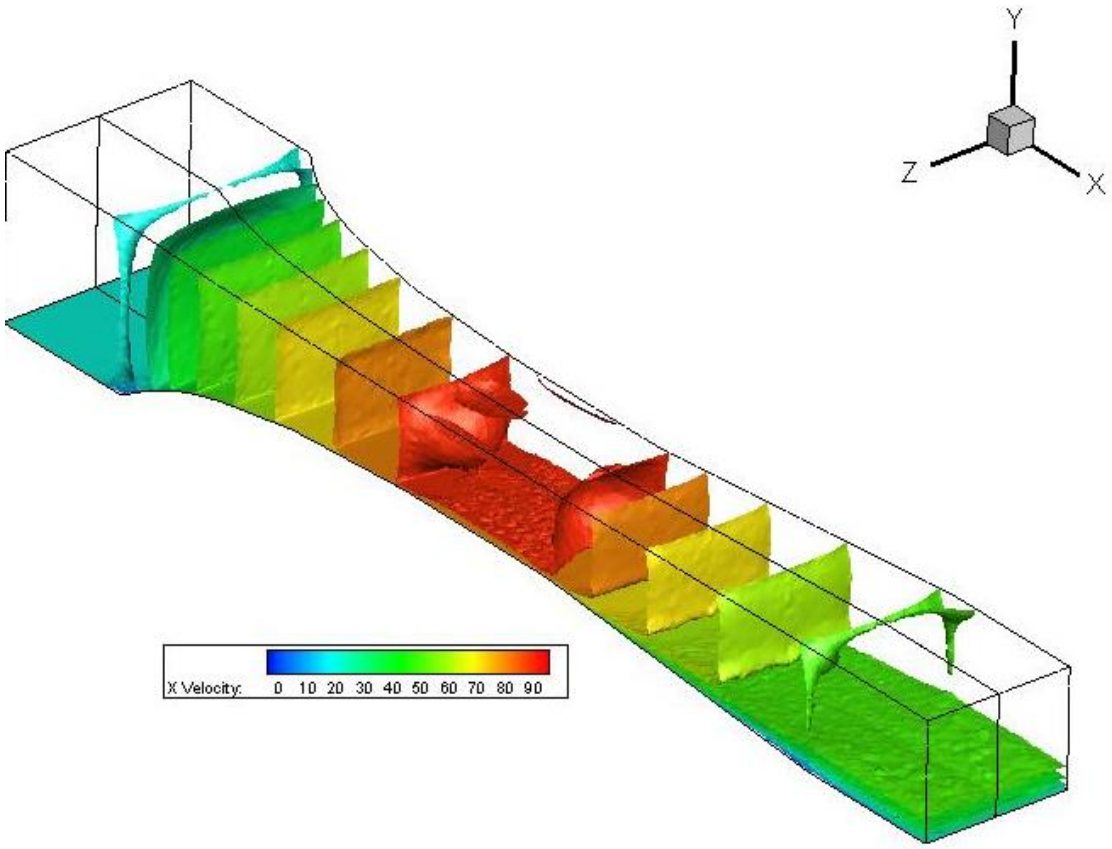

Figure 5-5. X velocity Isoplot

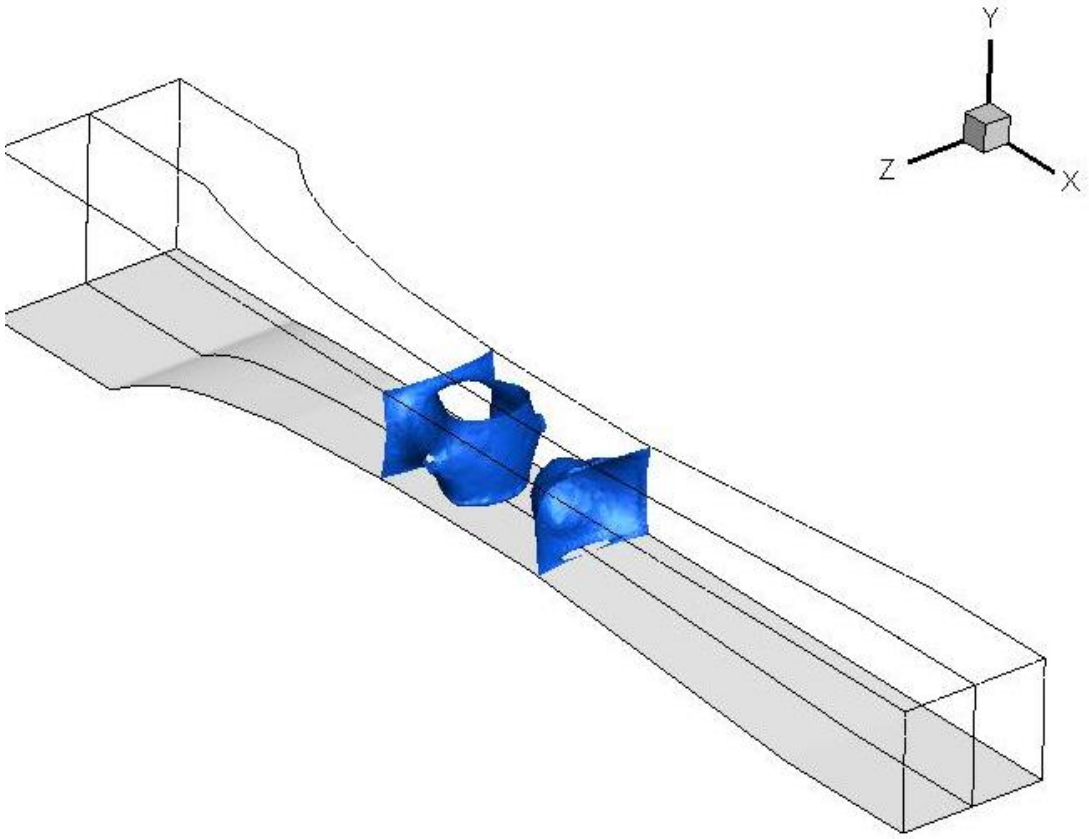

Figure 5-6. Pressure Isoplot p=97582 Pa

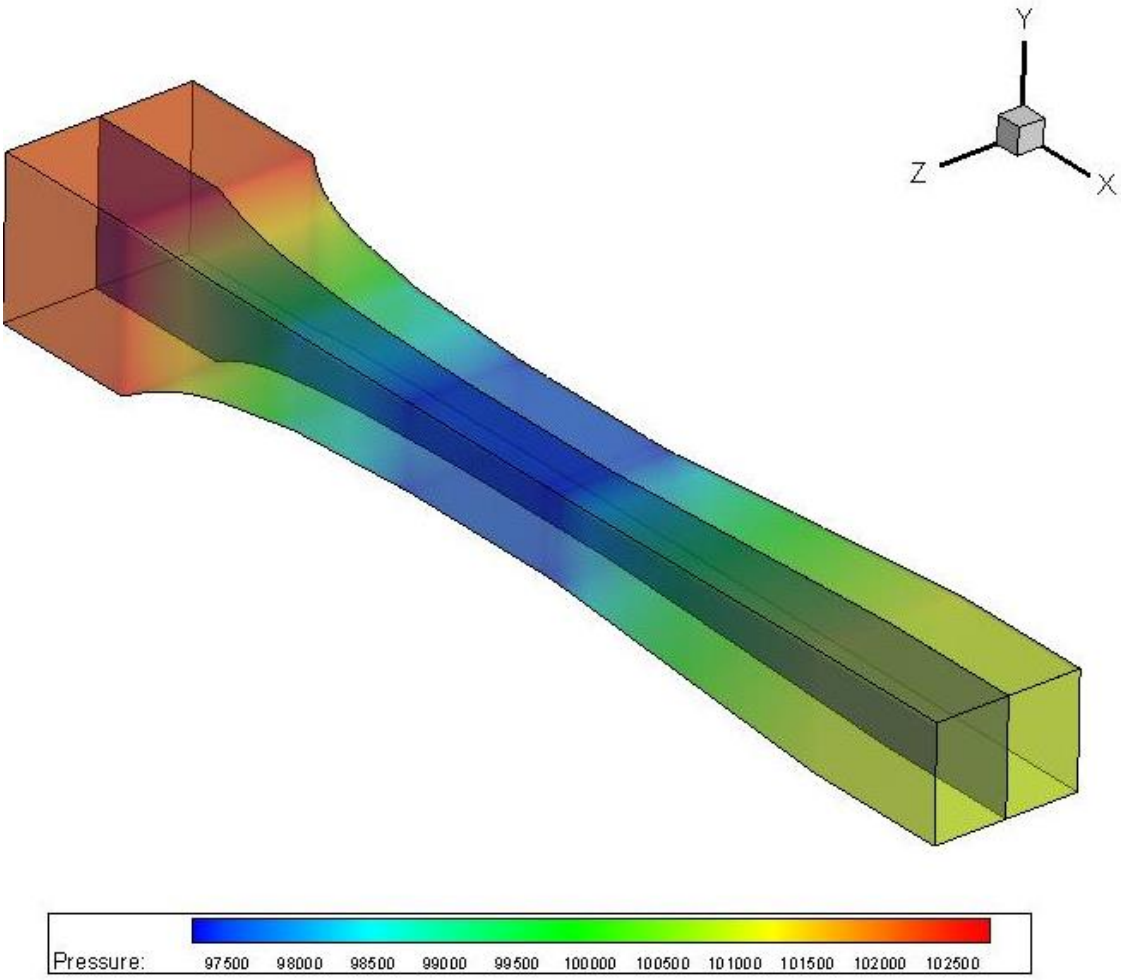

Figure 5-7. Pressure contour

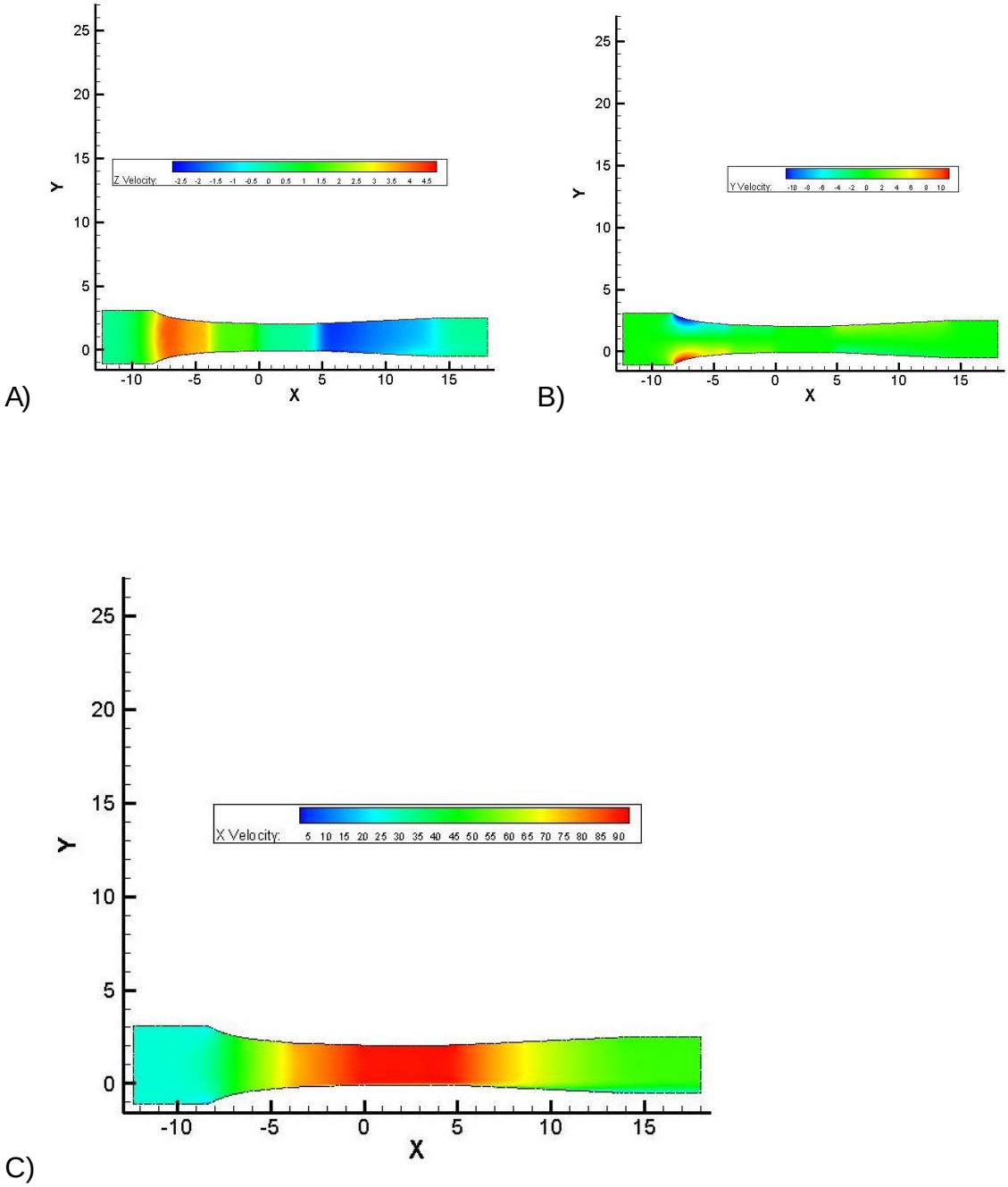

Figure 5-8. Velocity contours at the symmetry plane. A) W velocity B) V velocity C) U velocity

CHAPTER 6
GTS SIMULATION WITH RANS

Mesh and Physics

Medium mesh has been used for the simulation. Inflation layers have been added to the truck walls. The first layer thickness was 3e-6 m and 35 layers with 20% growth rate were added. The mesh was refined further at the point of contact between the supports and the road to reduce the skewness of the mesh. The outflow pressure obtained from boundary layer correction simulation was used.

The flow was assumed to be compressible and air was assumes as ideal gas. Density based solver was used to obtain the steady state solution. RANS k-w SST turbulence model was used. The flow was initialized with standard initialization from inlet and then FMG initialization was carried out. First order upwind scheme was used for first 100 iterations and then second order scheme was turned on. The steady state solution was obtained by reducing the residuals to less than 10e-6 and was also confirming by monitoring the pressure and velocity values at the reference point.

Results

The test section static pressure was 97575 Pa where as the empty tunnel simulation predicted 97582 Pa. So there was not much change in the pressure with the addition of GTS into the wind tunnel. Mach number at the test section was 0.269 which is same as experimental value. The drag at 0 degree yaw angle was calculated to be 0.35. The results can be seen in Table 6-1.

The x velocity contour in Figure 6-1 shows that there is uniform velocity in the test section. The velocity is low at the base of the truck and has couple of high velocity

regions in front of the truck. The pressure contour in Figure 6-2 shows the high pressure region in front of the truck with low pressure region at the rear. There are also a couple of low pressure regions, as the air flows from front to top and bottom surfaces of the truck, creating separation.

Vertical stream wise cut at the centerline of the base of the truck, near the wake region, along with the u, v velocity contours and streamlines can be seen in Figures 6-3 and 6-4. NASA experiment predicted a large counter clockwise rotating vortex which is centered at x/w= 8 , y/w=0.4. Also a clockwise vortex is suggested at the top right corner of PIV window. RANS simulations predicted a symmetric pair of vortices centered at x/w = 8. Figure 6-4 shows the vertical stream wise cut with v velocity contour. Also, the experiment predicts a high velocity region nearby the vortex centered at x/w=8.7, y/w=0.6. But RANS did not predict the high velocity region.

Figure 6-5 shows the pressure coefficient Cp, which is calculated with reference pressure, along the centerline of the truck. The Cp value could not be matched exactly with that of the experiment due to coarser nature of the mesh.

As we can see that, RANS failed to predict the wake structure behind the trailer. It predicted a symmetrical vortex structures where as the experiment predicted an asymmetrical vortex structures.

Table 6-1. RANS simulation results

Nodes	Elements/cells	inlet stagnation pressure (in Pa)	inlet stagnation temp (in K)	test static pressure (in Pa)	test velocity (in m/s)	Mach no	Outlet pressure (in Pa)	drag (full)	iteration	Pseudo time step (in sec)
501866	1282669	102653.2	282	97575	90.081	0.26962	101023	0.305	6703	0.001

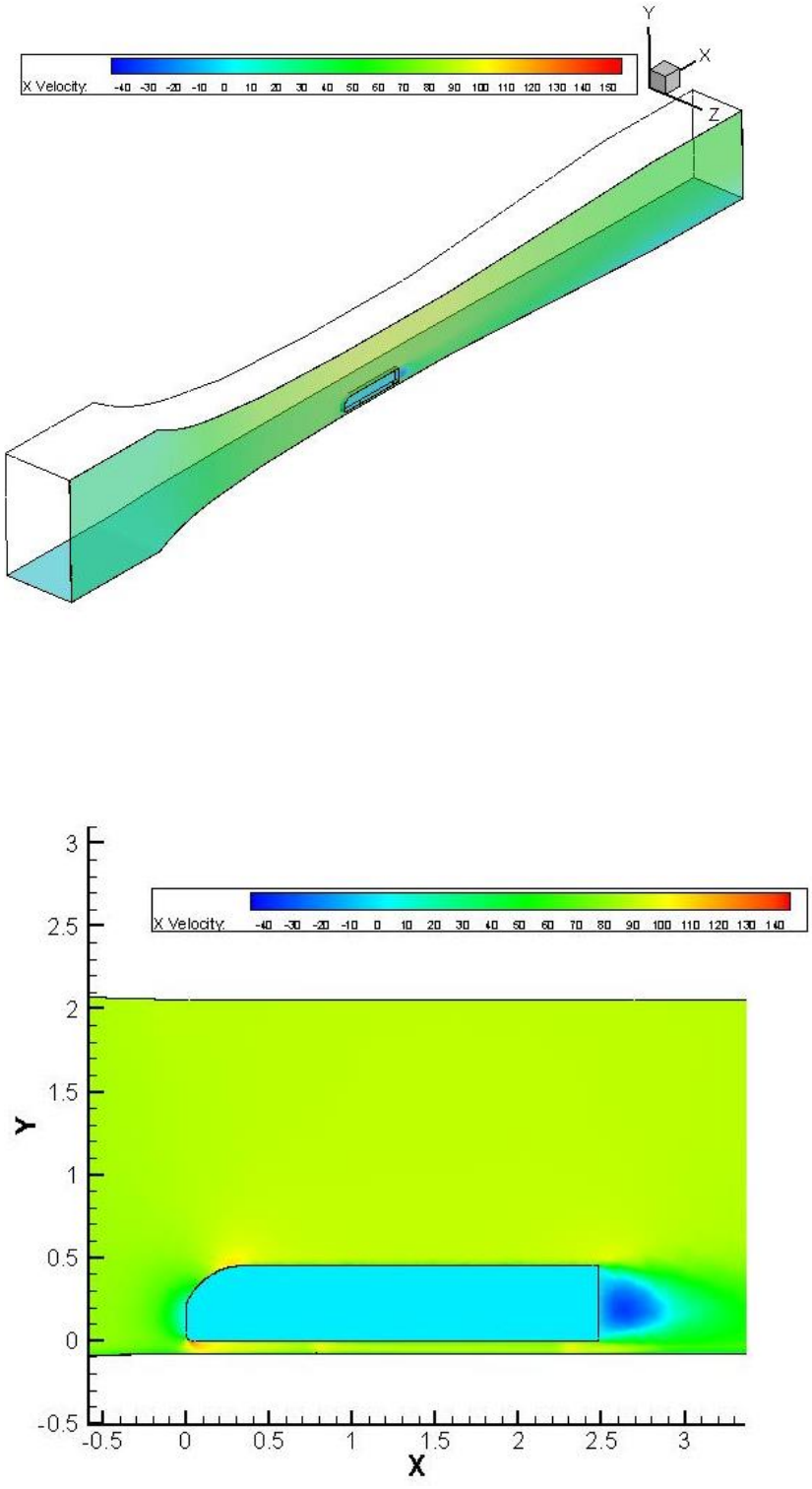

Figure 6-1. X Velocity contours at the symmetry plane

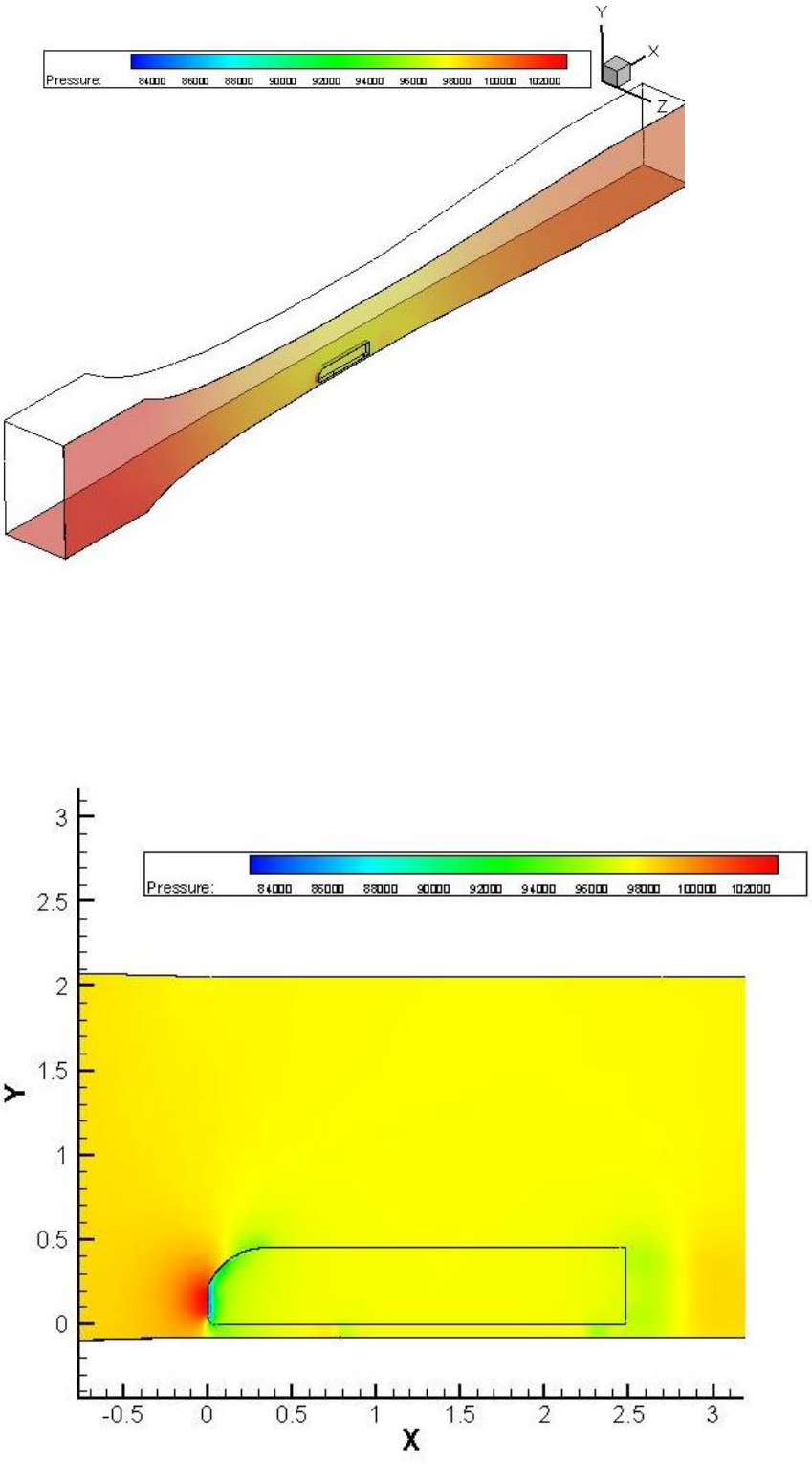

Figure 6-2. Pressure contours at the symmetry plane

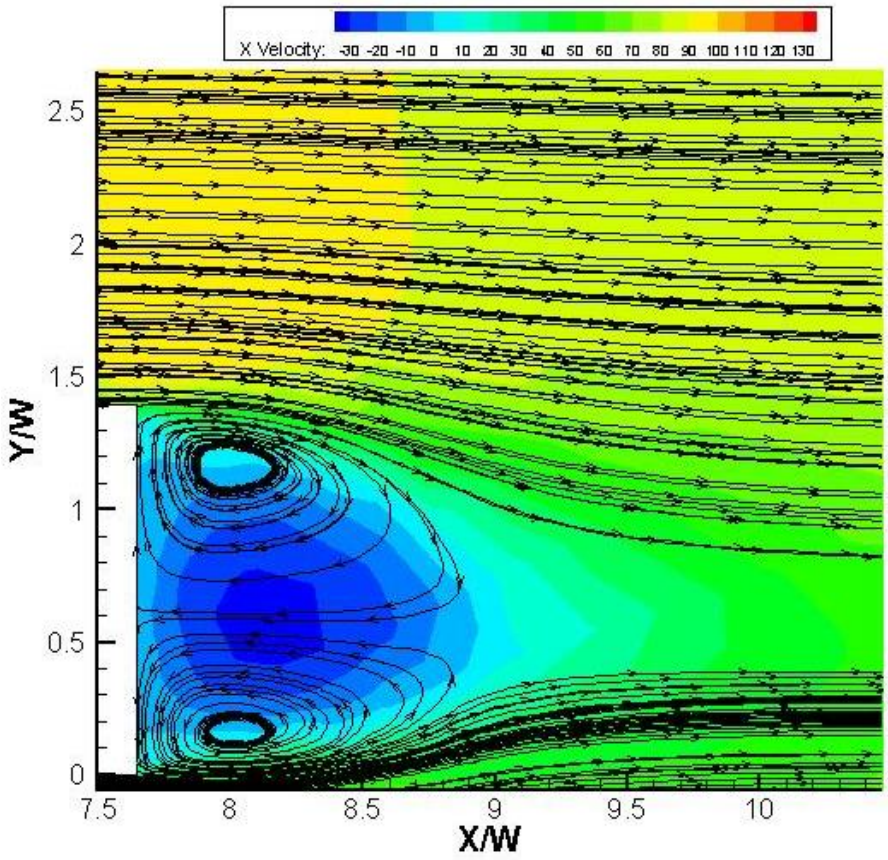

c)

Figure 6-3. Vortex structures at the base of the trailer with X velocity contour .

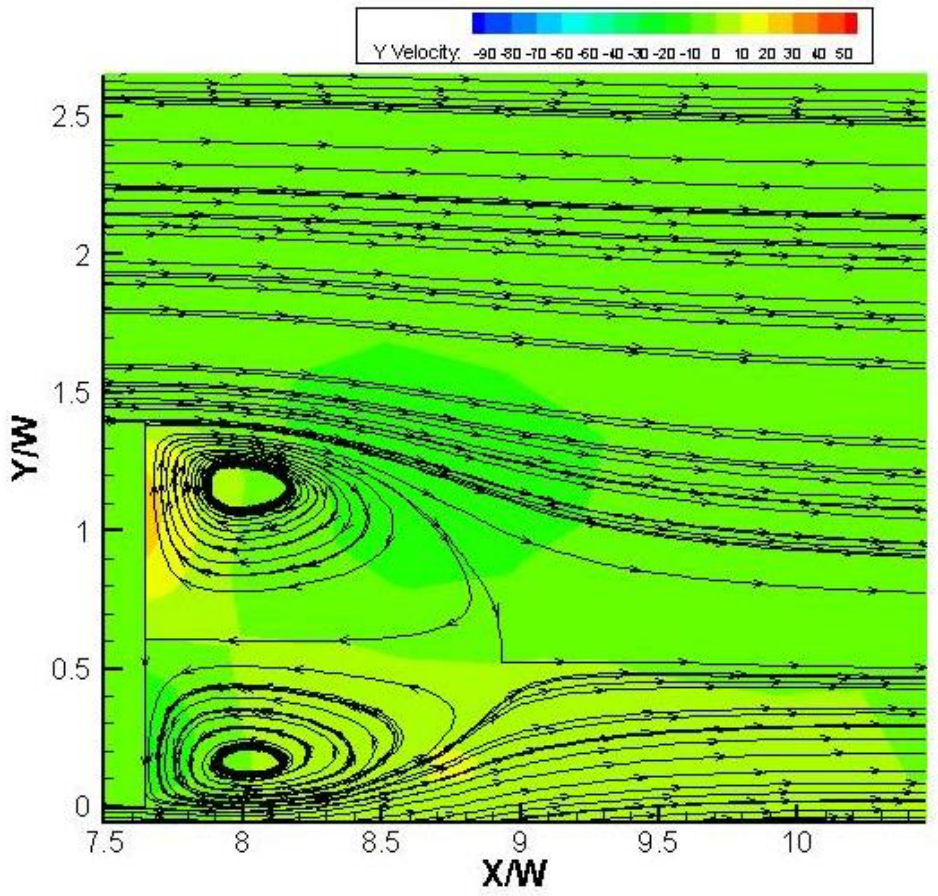

Figure 6-4. Vortex structures at the base of the trailer with Y velocity contour

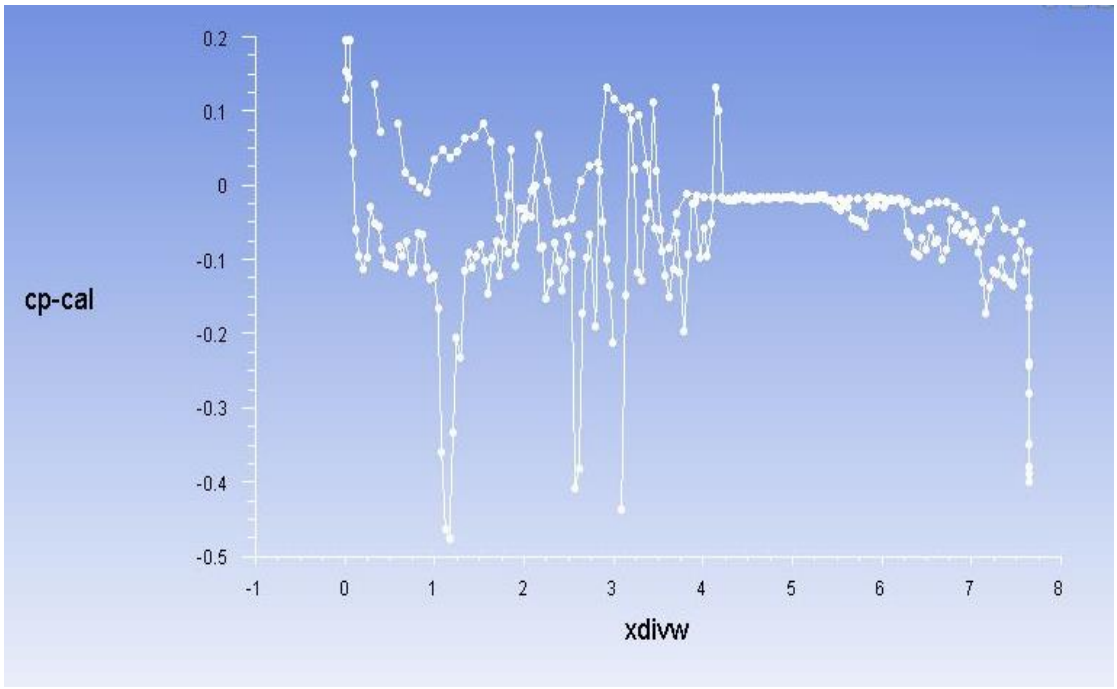

Figure 6-5. Cp at the centerline of the truck.

CHAPTER 7
GTS SIMULATION WITH DES

Mesh and Physics

The medium mesh which has been used for the GTS RANS simulation was used. The outflow pressure obtained from the boundary layer correction RANS simulation was applied.

The flow was assumed to be compressible and air was assumed as an ideal gas. DES with k-omega SST turbulence model was used. The flow was initialized with standard initialization from inlet. First order upwind scheme was used for first few iterations and then the second order scheme was turned on. Time step was started with 0.001 sec and was ramped upto 3sec. Each time step had 200 iterations. Courant number was also ramped up from 1 to 3.

Results

The simulation was run for 247 sec and the monitored values were oscillating between 2 bounds. The residuals were in the order of 10e-2 but the net mass flux was 3% of the inlet mass flux. So, the solution was assumed to have reached to the steady state. Figure 7-1 shows the results of the simulation. As the outlet pressure obtained from the RANS simulation was used, the pressure and the Mach number predicted at the reference point were 98362.5 Pa and 0.24894. But the test conditions in the experiment were 97582 Pa and 0.27. A drag coefficient of 0.24 was calculated. The lower velocity at the test section compared to the experimental value also contributed to the under prediction of the drag coefficient.

Figure 7-2 and Figure 7-3 shows the x velocity contour and pressure at the symmetry plane. Along with the wake behind the Trailer, there is a flow separation at the top of the truck creating a low pressure region.

Figure 7-4 shows the vortex structures at the base of the truck. There are 2 vortices, the top rotating in counter clockwise and the bottom one clockwise. The top vortex structure is large and is centered near the base of the truck. C.J.Roy et al. DES simulation[22] predicted that the size and nature of the vortex structures is highly dependent on the mesh. His simulation with coarse mesh with 3.8 million cells predicted two asymmetrical vortex structures while the refine mesh with 13.2 million cells predicted the symmetrical vortex structures. Importantly, none of the simulation predicted the wake similar to the experiment. This shows us that DES simulation has to be further studied.

Table 7-1. DES simulation results.

Nodes	Elements /cells	inlet stagnation pressure (in Pa)	inlet stagnation temperature (in K)	test static pressure (in Pa)	test velocity (in m/s)	Mach no	Outlet pressure (in Pa)	drag (full)	y+(road)
				98318	84.744	0.25338			
				98407	81.787	0.2445			
501866	1282669	102653.2	282	98362.5	83.2655	0.24894	101023	0.24	0 to 0.5

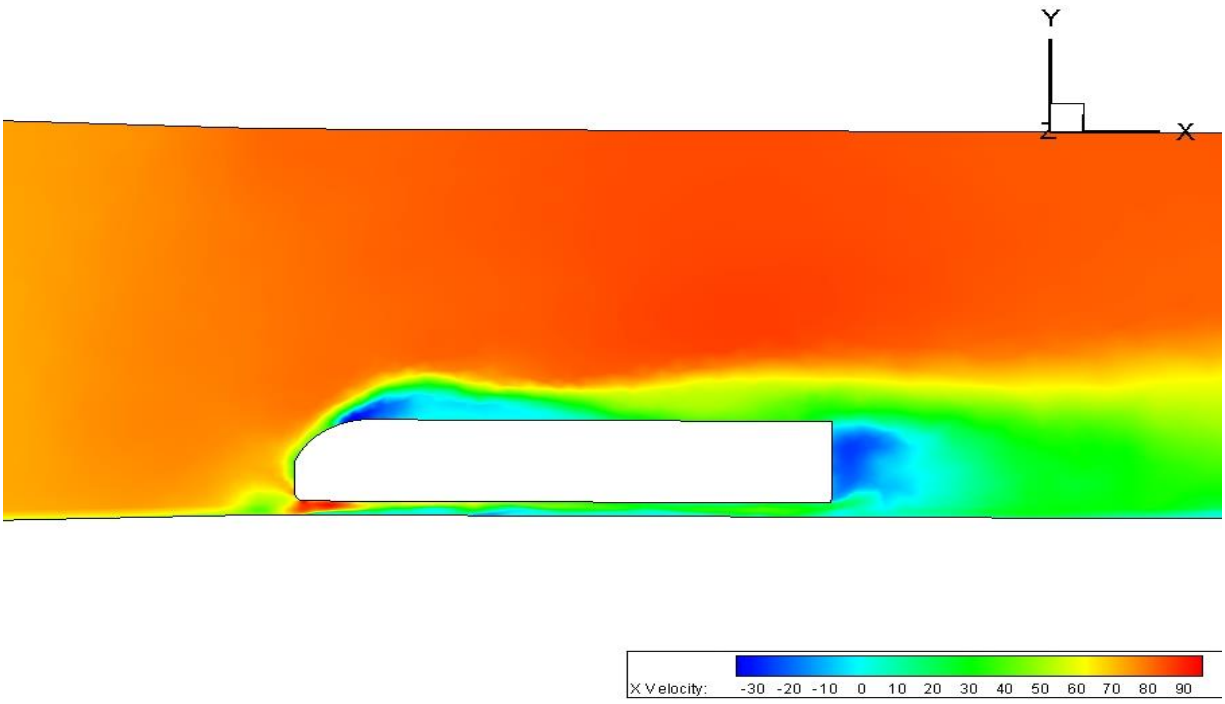

Figure 7-1. X velocity contour

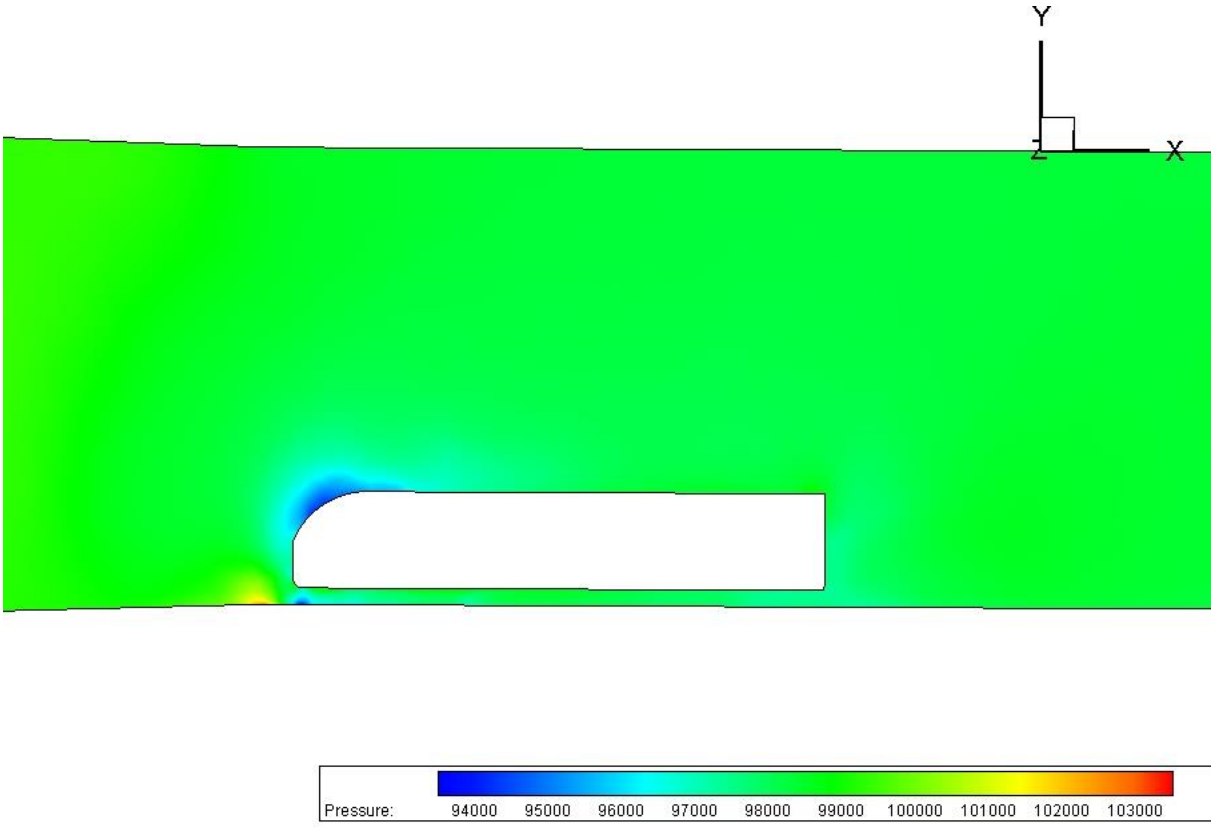

Figure 7-2. Pressure contour

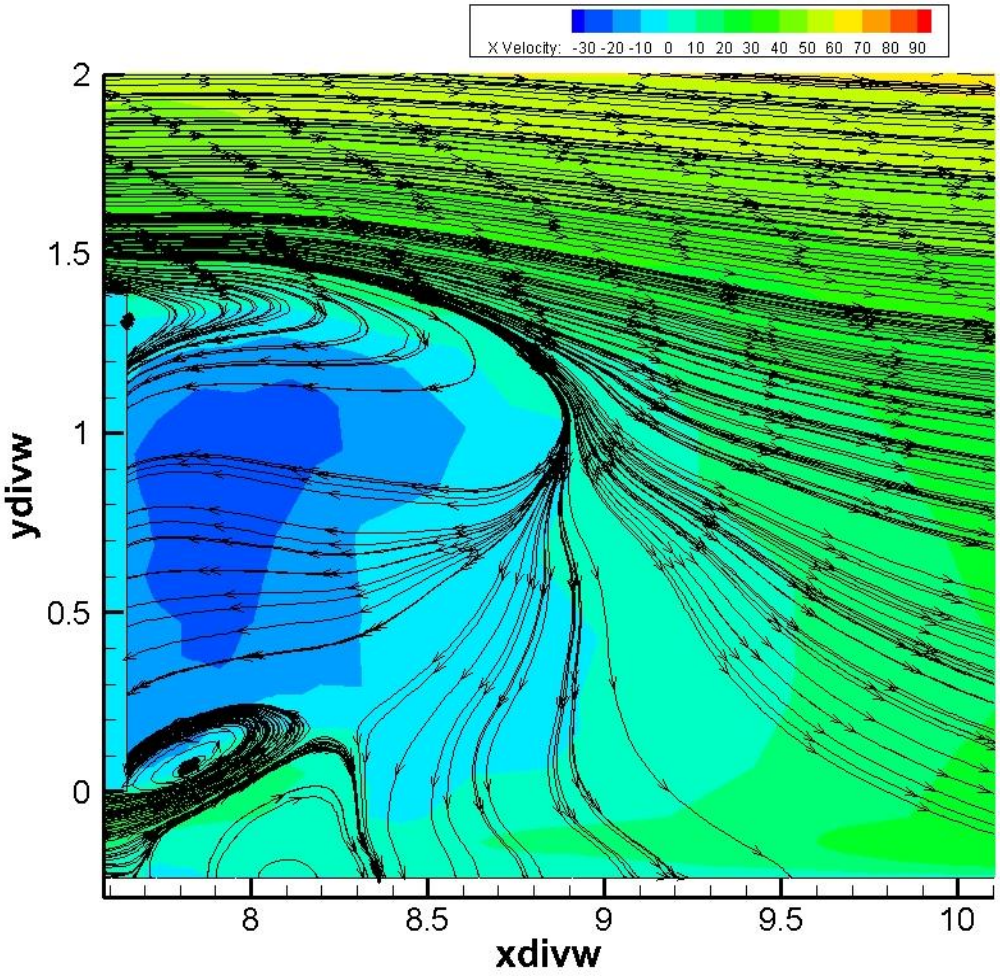

Figure 7-3. Vortex structures at the base of the trailer with X velocity contour

CHAPTER 8
CONCLUSION

RANS simulations showed clearly that they are not good enough for predicting the vortices structure behind the trailer. The results of the DES simulation were also not in accordance with the experimental results. But as the simulation was carried out on a coarse mesh due to computational resource limitation, it should be further investigated before moving onto LES turbulence model.

If the DES/LES simulations were able to predict the wake similar to that of the experiment then one can analyze the effect of boundary layer manipulating devices like Plasma actuators on the wake.

LIST OF REFERENCES

[1] S. C Davis and et.al, *Transportation Energy*. 2012.

[2] www.fhwa.dot.gov.

[3] W. D. Pointer, F. Browand, M. Hammache, T. Y. Hsu, M. Rubel, P. Chatalain, R. Englar, J. Ross, J. T. Heineck, S. Walker, D. Yaste, and B. Storms, "DOE ' s Effort to Reduce Truck Aerodynamic Drag-Joint Experiments and Computations Lead to Smart Design," AIAA Fluid Dynamics Conference ,2004.

[4] www.wikipedia.org

[5] J. Katz, "Aerodynamics of Race Cars," *Annual Review of Fluid Mechanics*, vol. 38, no. 1, pp. 27–63, Jan. 2006.

[6] D. J. Bush, "STREAMLINING AND AMERICAN INDUSTRIAL DESIGN," ," The MIT Press vol. 7, no. 4, pp. 309–317, 1974.

[7] K. R. Cooper, "Commercial Vehicle Aerodynamic Drag Reduction : Historical Perspective as a Guide," Applied and Computational Mechanics ,2012.

[8] J. Ortega, K. Salari, and B. Storms, "Investigation of Tractor Base Bleeding for Heavy Vehicle Aerodynamic Drag Reduction," 2009.

[9] K. R. Cooper and J. Leuschen, "Model and Full-Scale Wind Tunnel Tests of Second-Generation Aerodynamic Fuel Saving Devices for Tractor-Trailers," 2005.

[10] B. L. Storms, D. R. Satran, J. T. Heineck, and S. M. Walker, "A Summary of the Experimental Results for a Generic Tractor-Trailer in the Ames Research Center 7- by 10-Foot and 12-Foot Wind Tunnels," no. NASA/TM July, 2006.

[11] G. M. R. Van Raemdonck and M. J. L. Van Tooren, "DESIGN OF AN AERODYNAMIC AID FOR THE UNDERBODY OF A TRAILER WITHIN A TRACTOR-TRAILER COMBINATION," BBAA VI International Colloquim on Bluff Body Aerodynamics pp. 20–24, 2008..

[12] R. M. Wood, "Impact of Advanced Aerodynamic Technology on Transportation Energy Consumption," SAE International, 2004.

[13] J. Leuschen and K. R. Cooper, "Summary of Full-Scale Wind Tunnel Tests of Aerodynamic Drag-Reducing Devices for," Springer, Applied and Computational Mechanics, Volume 41 , 2009..

[14] D. Pointer, T. Sofu, J. Chang, and D. Weber, “Applicability of Commercial CFD Tools for Assessment of Heavy Vehicle Aerodynamic Characteristics.” Springer, Applied and Computational Mechanics, Volume 41 , 2009

[15] R. C. Mccallen, K. Salari, J. Ortega, and L. J. Dechant, “FY2003 Annual Report : DOE Project on Heavy Vehicle Aerodynamic Drag,” Lawrence Livermore National Laboratory reports,2003.

[16] K. Salari and J. Ortega, “Aerodynamic Design Criteria for Class 8 Heavy Vehicles Trailer Base Devices to Attain Optimum Performance,” Lawrence Livermore National Laboratory reports,2010.

[17] D. G. Hyams, K. Sreenivas, R. Pankajakshan, D. Stephen Nichols, W. Roger Briley, and D. L. Whitfield, “Computational simulation of model and full scale Class 8 trucks with drag reduction devices,” *Computers & Fluids*, vol. 41, no. 1, pp. 27–40, Feb. 2011.

[18] J. Leuschen and K. R. Cooper, “Full-Scale Wind Tunnel Tests of Production and Prototype , Second-Generation Aerodynamic Drag-Reducing Devices for,” SAE International, 2006.

[19] Bruce L Storms et al., “An Experimental System Study of the Ground Model Transportation (GTS) in the NASA Ames 7- by 10-Ft Wind,” NASA NTRS, 2001.

[20] K. Salari, “Computational Flow Modeling of a Simplified Integrated Tractor-Trailer Geomety,” Lawrence Livermore National Laboratory reports, September, 2003..

[21] C. J. Roy, J. Payne, and M. McWherter-Payne, “RANS Simulations of a Simplified Tractor/Trailer Geometry,” *Journal of Fluids Engineering*, vol. 128, no. 5, p. 1083, 2006.

[22] C. J. Roy and H. A. Ghuge, “Detached Eddy Simulations of a Simplified Tractor / Trailer Geometry.” Springer, Applied and Computational Mechanics, Volume 41 , 2009.

BIOGRAPHICAL SKETCH

Vikram Manthri was born in Andhra Pradesh, India. He completed his Bachelor of Technology in Mechanical Engineering from National Institute of Technology (NIT), Kurukshetra, Haryana, India in June 2008. Later on, he worked in Reliance Infrastructure Limited as Assistant Manager until June 2011. In August 2011, he joined University of Florida to pursue his master's in mechanical engineering. He got the opportunity to work with Dr. Subrata Roy and Dr. H.A. Ingley in spring 2013 and then worked in Applied Physics Research Group. After completing his master's, Vikram plans to contribute to the engineering industry.